Regorafenib analogues and their ferrocenic counterparts: synthesis and biological evaluation

Myron Wilde, Danielle Arzur, Blandine Baratte, Dorian Lefebvre, Thomas Robert, Thierry Roisnel, Catherine Le Jossic-Corcos, Stéphane Bach, Laurent Corcos, William Erb

Regorafenib analogues and their ferrocenic counterparts: synthesis and biological evaluation

Myron Wilde,[a] Danielle Arzur,[b] Blandine Baratte,[c,d] Dorian Lefebvre,[c,d] Thomas Robert,[c,d] Thierry Roisnel,[a] Catherine Le Jossic-Corcos,[b] Stéphane Bach,*[c,d] Laurent Corcos*[b] and William Erb*[a]

Approved by the FDA in 2012, Regorafenib is one of the last chance treatments for colorectal cancer. While various analogues have already been prepared, ferrocenic derivatives have never been evaluated. In this study, we prepared various ferrocene-containing derivatives of Regorafenib and recorded their biological activity in kinase and cellular assays. This led to the identification of a squaramide derivative which shows a good cellular activity and three ferrocene analogues with promising activity in both kinase and cellular assays.

Introduction

Cancer is an ongoing major worldwide public health concern with more than eighteen million newly diagnosed cases in 2018.[1] Together with surgery and radiotherapy, chemotherapy remains one of the main treatments, especially for metastatic and aggressive cancers.

While the medicinal chemistry programs were mainly dedicated to the search for cytotoxic chemotherapeutics in the 20th century, the advances made in molecular biology revolutionized chemotherapy. Indeed, the discovery of oncogenes and the understanding of signal transduction pathways allowed the emergence of new therapeutic targets such as kinases.[2] Launched on the market in 2001, Imatinib was the first small-molecule kinase inhibitor approved by the FDA for the management of chronic myelogenous leukemia.[3, 4] While this drug was developed to selectively target the Bcr-Abl fusion protein, it has been later proposed that targeting multiple kinases implicated in both tumour cell proliferation and angiogenesis could be a relevant cancer therapy.[5, 6] This was nicely illustrated with the development of sunitinib and sorafenib, two multiple kinase inhibitors targeting vascular endothelial growth factor receptor (VEGFR), platelet-derived growth factor receptor (PDGFR), Fms-like tyrosine kinase 3 receptor (flt3), the cytokine receptor kit, including an additional downstream of the Raf/MEK/ERK pathway for the latter.[7, 8]

Colorectal cancer currently represents close to 10% of the diagnosed cancers and deaths worldwide and is considered to be the fourth most deadly.[9, 10] While surgery currently remains the main curative treatment for localized tumours, its combination with chemotherapeutic agents such as fluoropyrimidines and oxalilplatin is recommended for advanced cases.[9, 10]

[a] Univ Rennes, CNRS, ISCR (Institut des Sciences Chimiques de Rennes) - UMR 6226, F-35000 Rennes, France. E-mail: william.erb@univ-rennes1.fr
[b] INSERM, UMR 1078, Université de Brest, Génétique Génomique Fonctionnelle et Biotechnologies, Etablissement Français du Sang, Brest, France. E-mail: laurent.corcos@univ-brest.fr
[c] Sorbonne Université, CNRS, FR 2424, Plateforme de criblage KISSf (Kinase Inhibitor Specialized Screening facility), Station Biologique de Roscoff, 29680 Roscoff, France. E-mail: bach@sb-roscoff.fr
[d] Sorbonne Université, CNRS, UMR 8227, Laboratory of Integrative Biology of Marine Models (LBI2M), Station Biologique de Roscoff, 29680 Roscoff, France.

Regorafenib (**1a**) is a newly-approved drug for the treatment of metastatic colorectal cancer (Fig 1). Indeed, this fluorinated analogue of sorafenib displayed an improved activity profile, targeting both key angiogenic (VEGFR, PDGFR, Tie2) and tumorigenic (Kit, Ret, Raf) kinases.[11-13] Based on its structure, it is classified as a type II inhibitor, as it is believe to bind to the inactive form of the kinase.[14, 15] As for the other type II inhibitors, the pyridine ring fits in the ATP binding pocket and interacts with the hinge region in a bidentate fashion while the lipophilic (trifluoromethyl)phenyl ring occupies an allosteric site. Finally, as observed with sorafenib, the urea motif is likely to develop additional H-bonds to stabilize the molecule in the active site.

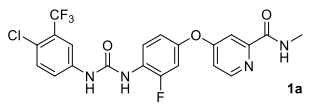

Fig 1. Regorafenib (**1a**).

Although many analogues of both sorafenib and regorafenib have been prepared and their biological properties evaluated in various studies,[16-24] to the best of our knowledge, no ferrocene derivatives have been reported to date. In the field of bioorganometallic chemistry, the derivatization of a biologically active compound with an organometallic part is an attractive approach to reach original properties.[25-31] While the incorporation of ferrocene into a drug can be traced back to 1960,[32] it is in the late nineties that the most popular examples of this strategy emerged. In 1996, the group of Jaouen reported the synthesis of ferrocene derivatives of the anticancer agent tamoxifen, the so-called ferrocifens.[33] In addition to a similar activity against hormone-dependent breast cancer cells, the new molecules were also active against hormone-independent ones. In the following years, many derivatives with increased activity were prepared and the ferrocifens family currently encompassed more than 200 members.[29, 34-36] In 1997, the team of Biot reported the synthesis of ferroquine, a ferrocene derivative of the antimalaria drug chloroquine with an improved bioactivity against chloroquine-resistant strains of *Plasmodium falciparum*.[27, 37, 38] This led to the development of this molecule into a drug, currently in clinical trials. More recently, ferrocene analogues of antifungal and antiparasitic drugs were successfully prepared and showed promising bioactivities.[39-44]

In bioorganometallic chemistry, ferrocene can play multiple roles. It can act as a simple bulky isostere that would fit into a hydrophobic pocket of the target to improve its binding affinity.[45] It can also act as an electron relay to promote the transformation of a prodrug into its active form as noticed with the ferrocifen family.[29] Ultimately, ferrocene is able to generate reactive oxygen species (ROS) in biological media as observed for ferroquine.[46]

To the best of our knowledge, the inhibition of a kinase implicated in colorectal cancer with a molecule incorporating a ferrocene has only been investigated in the group of Spencer who reported the syntheses of simplified analogues of sunitinib and erlotinib.[47, 48] While their biological evaluation revealed the inhibition of VEGFR and epithelial growth factor receptor (EGFR), an important loss of activity was noticed when compared to the parent drug. Interested in both ferrocene chemistry[49-57] and the synthesis of biologically active products,[58-63] we report in the present study how to reach ferrocene derivatives of non-truncated kinase inhibitors as well as their early biological evaluation in both enzymatic and cellular assays.

Results and discussion

Syntheses of the targeted compounds

Acting as a multi-kinase inhibitor, we selected regorafenib as the reference drug and expected original switches of activity and selectivity upon the introduction of the ferrocene core. We also explored the replacement of the urea by a bioisostere and selected squaramide and oxalyl amide.[64, 65] Indeed, although such derivatives of sorafenib were previously described,[66, 67] their biological properties were not reported. Therefore, regorafenib (**1a**), its squaramide (**1b**) and oxalyl amide (**1c**) derivatives were defined as our first targets (Fig 2). Concerning ferrocene analogues, we decided to focus our efforts on the replacement of the trifluoromethylated phenyl ring as it fits into a hydrophobic pocket that would accommodate the bulky ferrocene core and thus designed the compounds **2a-c** and **3a-c**. Finally, we also included the derivatives **4a-b** and **5a-b** in our study as the *N*-substituent of the carboxamide is exposed to the solvent and therefore not limited in terms of steric volume.

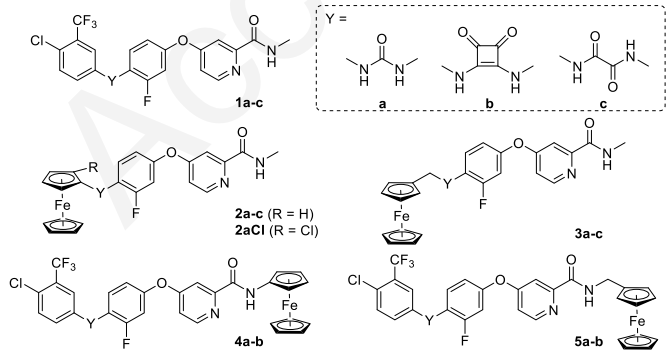

Fig 2. Synthetic targets of the present study.

While most of the syntheses of regorafenib start with 4-amino-3-fluorophenol, we planned to access the targeted compounds **1-3** from the aniline **6** by reaction with a suitable partner (Scheme 1). This key aniline was to be prepared by following the nitration-reduction sequence reported by Zhai and Gong from **7**,[68] accessible by a nucleophilic aromatic substitution from 3-fluorophenol (**8**) and the 4-chloropyridine derivative **9**.

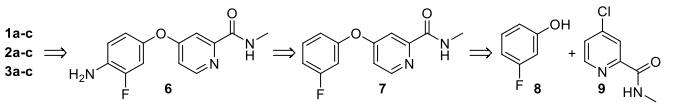

Scheme 1. Retrosynthetic analysis.

The reaction of picolinic acid (**10**) with the Vilsmeier reagent, formed in situ from thionyl chloride and catalytic dimethylformamide (DMF), afforded the acyl chloride **11** which was reacted with methylamine to deliver the carboxamide derivative **9** in a 46% overall yield (Scheme 2).[69] It was then reacted with 3-fluorophenol (**8**) in DMF in the presence of potassium *tert*-butoxide and a catalytic amount of potassium carbonate to give the ether **7** (61% yield). The nitration of **7** was reported by Zhai and Gong to be highly regioselective toward the *para* isomer.[68] However, in our hands and despite many attempts, the *ortho* isomer was invariably formed as a by-product while full conversion was never reached. Consequently, we obtained an inseparable mixture of ***p*-12**, ***o*-12** and starting material **7** in a 1:0.7:0.3 ratio. Fortunately, subjecting this mixture to an acidic iron-mediated nitro reduction allowed pure aniline **6** to be isolated in a moderate 20% yield over the 2 steps.[68]

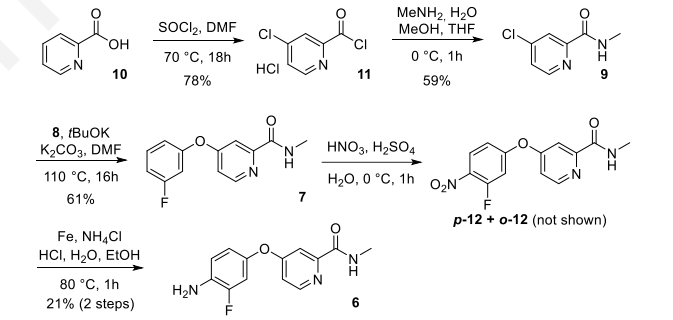

Scheme 2. Syntheses of the aniline **6**. DMF: dimethylformamide.

1-Chloro-2-(trifluoromethyl)benzene (**13**) was in turn nitrated toward the derivative **14**,[70] isolated in a 86% yield after recrystallisation to remove the undesired *ortho* isomer (Scheme 3, top). Iron-mediated reduction of the nitro group in the same conditions as before afforded the other required aniline **15** in an 81% yield. The aniline **15** was then reacted with triphosgene in the presence of *N*,*N*-diisopropylethylamine to deliver the corresponding isocyanate,[71] which was directly engaged into the urea formation upon the addition of the aniline **6** (Scheme 3, bottom). From this reaction, regorafenib (**1a**) was isolated in a 65% yield.

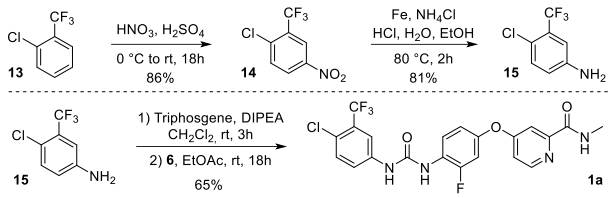

Scheme 3. Syntheses of the aniline **15** and regorafenib (**1a**). DMF: dimethylformamide.

We next focused our attention onto the original analogues **1b** and **1c**. Therefore, squaric acid (**16**) was first reacted with trimethylorthoformate to deliver **17** in an 84% yield (Scheme 4, top).[72] This dimethoxysquarate was engaged in a first substitution in the presence of the aniline **15** (intermediate **18**, 76% yield),[73] followed by a second substitution with the aniline **6** toward the final compound **1b**, obtained in a 24% yield. For electronic or steric reasons, the second substitution appeared disfavoured and required harsher reaction conditions. To progress toward the oxamide derivative, the aniline **15** was reacted with ethyl chlorooxoacetate in basic conditions toward **19** (87% yield),[66] which was saponified to deliver the corresponding carboxylic acid **20** in a 62% yield (Scheme 4, bottom).[66] Coupling **20** and the aniline **6** was lastly performed in the presence of hydroxybenzotriazole (HOBt), HBTU and *N*,*N*-diisopropylethylamine to deliver the oxamide **1c** in a 33% yield.[66] It is worth to mention the low solubility of **1c** in organic solvents, except dimethylsulfoxide.

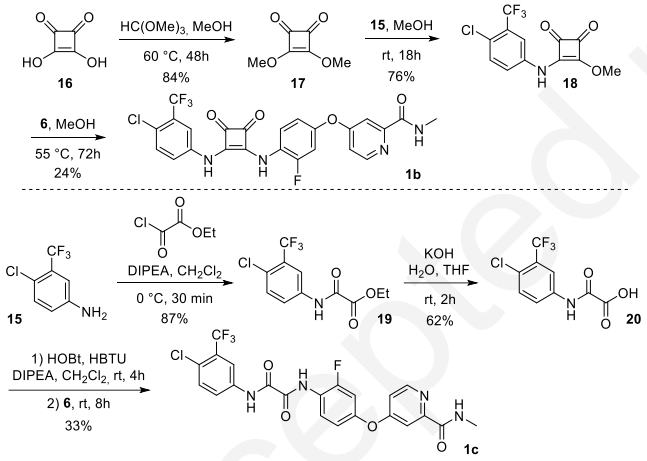

Scheme 4. Syntheses of the analogues **1b** and **1c**. DIPEA: *N,N*-diisopropylethylamine, HOBt: hydroxybenzotriazole, HBTU: *N,N,N',N'*-tetramethyl-*O*-(1*H*-benzotriazol-1-yl)uronium hexafluorophosphate.

With the first targets **1a-c** in hand, we next moved to the synthesis of the urea-based organometallic derivatives **2a** and **3a**. Concerned with the use of toxic triphosgene for the urea preparation, we briefly evaluated alternative approaches. To this goal, azidocarbonylferrocene (**21**) was engaged in a Curtius rearrangement to prepare the required isocyanate in situ (Scheme 5, top).[74] While the rearrangement occurred upon heating, only trace amount of product **2a** was noticed. As similar approaches have been reported twice to prepare regorafenib,[75, 76] we suspected that the weak electrophilicity of ferrocene isocyanate disfavoured the addition of the aniline and that decomposition pathways might became predominant. We also briefly studied the possibility to start from (aminomethyl)ferrocene (**22**)[77] and follow the carbonyldiimidazole route to form the urea (Scheme 5, top).[22] However, whatever the reaction conditions used, only mixtures of starting materials and unidentified degradation products were obtained. Similarly, formation of an intermediate carbamate as urea precursor was evaluated,[78] but this afforded **3a** in an unreproducible 40% yield. Although these results are difficult to rationalize, the electron-rich nature of ferrocene and its redox behaviour might be at the origin of unexpected degradation in the applied reaction conditions. The recourse to triphosgene was evaluated at last and, from (aminomethyl)ferrocene (**22**) and aminoferrocene (**23**),[79] the title products **2a** and **3a** were isolated in moderate 49% and 48% yields, respectively (Scheme 5, bottom).

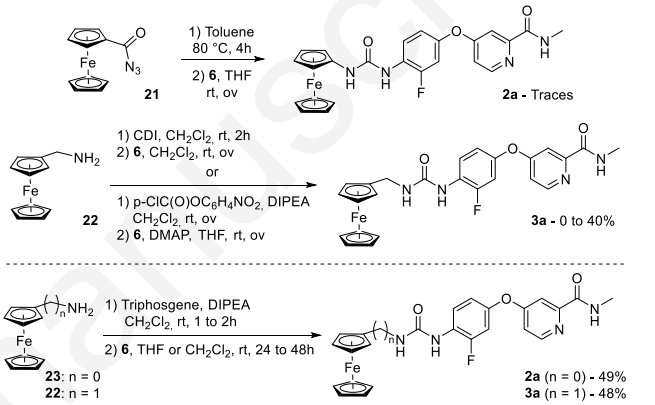

Scheme 5. Syntheses of the analogues **2a** and **3a**. CDI: carbonyldiimidazole, DIPEA: *N,N*-diisopropylethylamine, DMAP: 4-(dimethylamino)pyridine, THF: tetrahydrofuran.

Regorefanib features a 4-chloro-3-(trifluoromethyl)phenyl ring that fits into a hydrophobic pocket of the kinase. To mimic this lipophilic moiety, we wanted to introduce halogens onto the ferrocene core of compound **2a**. However, there is currently no reported routes toward either 1-amino-3-chloroferrocene or substituted trifluoromethylated ferrocene derivatives. Therefore, to validate our strategy we initially planned to introduce a chlorine next to the urea as depicted on scheme 6. To this goal, ferrocene was engaged into two deprotometallation-electrophilic trapping sequences, using hexachloroethane (compound **24**, 85% yield) and carbon dioxide (compound **25**, 78% yield) as electrophiles.[80, 81] The acyl azide **26** was easily prepared from the carboxylic acid **25** and diphenylphosphoryl azide and was then engaged into a Curtius rearrangement in the presence of *tert*-butanol to afford the original ferrocene **27** in a 91% yield. Carbamate deprotection, in situ formation of the corresponding isocyanate and addition of compound **6** were done in a stepwise manner to deliver the derivative **2aCl** in a 33% yield.

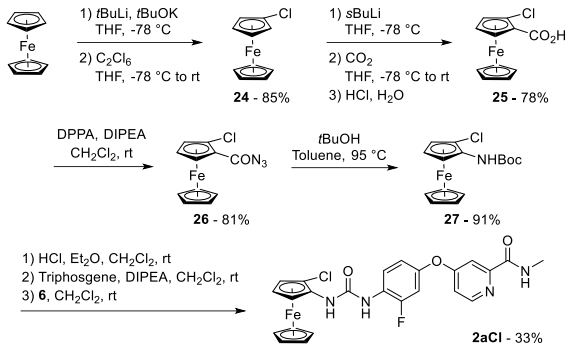

Scheme 6. Synthesis of the chlorinated analogue **2aCl**. DIPEA: *N,N*-diisopropylethylamine, DPPA: diphenylphosphoryl azide, THF: tetrahydrofuran.

With the ferrocene urea-based compounds in hand, we next moved to the squaramide derivatives **2b** and **3b**. In a first approach, we first reacted the methoxysquarate **17** with the aniline **6** toward **28**,[73] which was directly engaged in the second substitution in the presence of either (aminomethyl)ferrocene (**22**) or aminoferrocene (**23**) (Scheme 7, top). However, only decomposition products were obtained by following this approach. We decided to reverse the step order and therefore reacted **22** and **23** with the dimethoxysquarate **17** and isolated the intermediates **29** and **30** in low 20% and 34% yields, respectively (Scheme 7, bottom). This difference probably results from the increased stability of **22** when compared to **23**. However, whatever the reaction conditions used, we only observed decomposition products during the attempts to prepare the products **2b** and **3b** at higher temperatures. As we previously observed that the formation of the squaramide **1b** required harsh conditions, this disappointing reaction outcome probably results from the thermal instability of the ferrocene derivatives **29** and **30**.

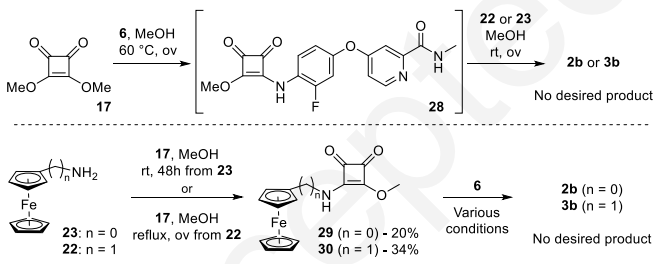

Scheme 7. Approach toward the analogues **2b** and **3b**. THF: tetrahydrofuran.

Contrary to the synthesis of the squaramide, the preparation of the ferrocene derivatives of oxalyl amide **2c** and **3c** was much simpler. Aminoferrocene (**23**) and (aminomethyl)ferrocene (**22**) were reacted with ethyl chlorooxoacetate in the presence of *N,N*-diisopropylethylamine[66] to deliver the amides **31** and **32** in 55% and 73% yields, respectively (Scheme 8). The higher yield noticed for the formation of the latter could be explained by the higher stability of **22** when compared to **23**. Saponification delivered the carboxylic acids **33** and **34**, which were reacted with the aniline **6** in the presence of HBTU as a coupling reagent to deliver the target compounds.[66] While **2c** was isolated in a moderate 51% yield, we only obtained **2d** in a disappointing 16% yield, which could be linked with the low solubility of the reagent in the coupling conditions.

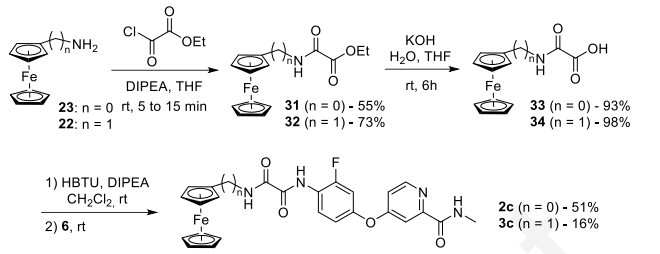

Scheme 8. Approach toward the analogues **2c** and **3c**. DIPEA: *N,N*-diisopropylethylamine, HBTU: *N,N,N',N'*-tetramethyl-*O*-(1*H*-benzotriazol-1-yl)uronium hexafluorophosphate, THF: tetrahydrofuran.

To reach our two final targets **4a-b** and **5a-b** with the ferrocene core attached to the carboxamide, we first prepared the substituted pyridines **35** and **36** by reacting the acyl chloride **11** with the required amino compounds (Scheme 9, top). The reaction between 4-amino-3-fluorophenol (**37**) and the isocyanate formed in situ from the aniline **15** and triphosgene then afforded the urea **38a** in a 22% yield (Scheme 9, bottom). Similarly, the reaction between the methyl squarate **18** and **37** conducted to **38b**, isolated in a 60% yield. However, all attempts to reach our targets by reacting **38a-b** with **35** or **36** only led to recovery of starting materials or degradation in harsher conditions. Therefore, we decided to reverse the step order and firstly carried out the ether formation (Scheme 10). The reaction between the phenol **37** and either **35** or **36** in the presence of potassium *tert*-butoxide afforded the corresponding products **39** and **40** in 52% and 71% yields, respectively. Finally, the addition of the aniline **15** onto the corresponding isocyanates, formed in situ by reaction with triphosgene, conducted to the targeted compounds **4a** and **5a** in 33% and 28% yields, respectively.[82]

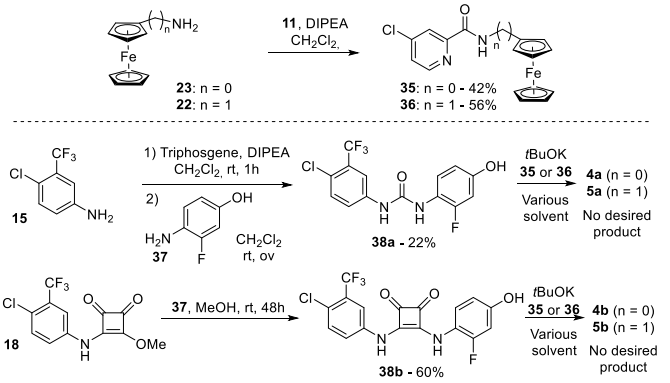

Scheme 9. Early attempts toward **4a-b** and **5a-b**. DIPEA: *N,N*-diisopropylethylamine.

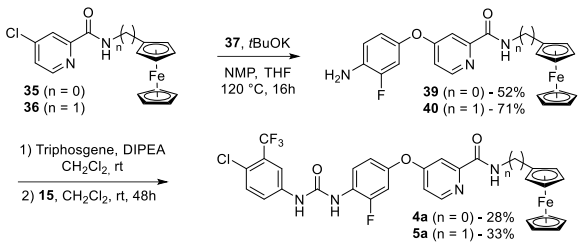

Scheme 10. Syntheses of compounds **4a** and **5a**. DIPEA: *N,N-diisopropylethylamine*, NMP: *N*-methylpyrrolidinone.

Crystals suitable for X-ray diffraction were obtained for compounds **6**, **7**, **19**, **31**, **35** and **39** by evaporation of their corresponding solutions. While the solid-state structures of the oxamides **19** and **31** were similar (Fig 3), interesting differences were noticed concerning the structures of compounds **6** and **7** (Fig 4). Indeed, while the picolinamide moieties are similar, the orientation of the fluorinated phenyl ring is different: bent downward for compound **7** while upward for compound **6**. This seems to result from a different hydrogen bonding network (see ESI). Indeed, for compound **7**, a H-bond between the amide NH of one molecule and the amide C=O of a second molecule was noticed. The additional amino group of compound **6** disrupted this organisation as the aniline NH was found to interact with the amide C=O, resulting in a structure in which the picolinamide and fluorinated phenyl ring of two molecules are head-to-tail (see ESI).

Fig 3. Left to right: molecular structure of compounds **19** and **31** (thermal ellipsoids shown at the 30% probability level).

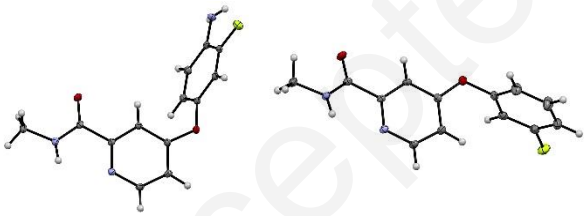

Fig 4. Left to right: molecular structure of compounds **6** and **7** (thermal ellipsoids shown at the 30% probability level).

Differences in the crystal structures of compounds **35** and **39** were also observed (Fig 5). Indeed, while the whole picolinamide moiety of compound **35** is almost coplanar with the substituted cyclopentadienyl ring, it is bent upward for compound **39**. Furthermore, for the latter, two molecules with various degrees of bending were observed in the asymmetric unit. Different hydrogen bonding interactions were also observed: while no H-bond was identified for compound **35**, it was found that the two forms of **39** that crystallize in the unit are in close contact through two H-bonds developed between aniline NH and amide C=O (see ESI).

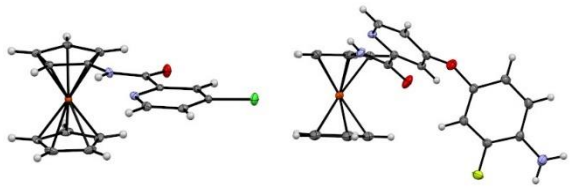

Fig 5. Left to right: molecular structure of compounds **35** and **39** (thermal ellipsoids shown at the 30% probability level). Only one form of **39** is shown.

Unfortunately, and despite our efforts, all the final compounds were obtained as amorphous solids, thus excluding X-ray structure determination. Therefore, they were fully characterized by different 1D (^{1}H and ^{13}C, DEPT) and 2D (COSY, HSQC, HMBC) NMR experiments (see ESI). The exploitation of HMBC experiment was particularly helpful to assign the NMR spectra and selected key correlations for compounds **1a**, **2aCl**, **2c** and **4a** are depicted on Fig. 6 (see ESI for selected HMBC correlations for the other compounds).

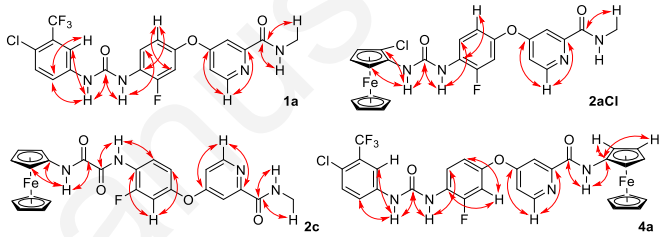

Fig 6. Selected HMBC correlations observed for compounds **1a**, **2aCl**, **2c** and **4a**.

Biological evaluation

Kinases inhibition. The parent drug regorafenib (**1a**) is known to act as a multi-kinase inhibitor (RTK, VEGFR1-3, TIE2, FEFR1, PDGFR-β; KIT, REF, cRaf, β-Raf). It has been reported that ferrocene derivatives of biologically active compounds can sometimes feature an original biological profile.[83, 84] Therefore, seeking a potential repurposing of regorafenib derivatives, we tested our compounds against a short panel of disease-related kinases for which regorafenib is not reported as a powerful inhibitor: cyclin-dependent kinases 5 (CDK5/p25) and 9 (CDK9/CyclinT), proto-oncogene kinase PIM1, CDC2-like kinase 1 (CLK1), dual specificity tyrosine phosphorylation regulated kinase 1A (DYRK1A), mitotic kinase Haspin, glycogen synthase kinase 3 (GSK3β) and casein kinase 1 (CK1ε). We also included four tyrosine kinases (vascular endothelial growth factor receptor VEGFR2, tyrosine-protein kinase ABL1, Janus kinase JAK3 and epithelial growth factor receptor EGFR) to evaluate the selectivity of the prepared compounds in this family. The inhibitory activities were determined at 10 and 1 µM (Tables 1 and 2, respectively). From this preliminary evaluation, it clearly appeared that none of the new regorafenib derivatives exhibits any off-target activity, except for the truncated squaramide derivative **38b**, acting as a weak PIM1 inhibitor at 10 µM. However, as expected, the best inhibitions were recorded on VEGFR2. While a clear drop of activity was obtained when replacing the urea by a squaramide or an oxamide (compounds **1a-c**), a ferrocene moiety can be tolerated, provided it is attached through a linker (compound **3a**) or substituted at the 2 position by a chlorine atom (compound **2aCl**).

Table 1 Inhibitory activities of the first round of compounds against a short panel of disease-related protein kinases. The table displays the remaining kinase activities detected after treatment with 10 µM of the tested compounds. Results are expressed in % of maximal activity, i.e. measured in the absence of inhibitor but with an equivalent dose of DMSO (solvent of the tested compounds). ATP concentration used in the kinase assays was 10 µmol/L (values are means, n = 2). Kinases are from human origin unless specified: *Mm*, *Mus musculus; Rn, Rattus norvegicus*. Data obtained for regorafenib (**1a**) are colored in light grey.

Compd.	CDK5/p25	CDK9/CyclinT	PIM1	*Mm*CLK1	*Rn*DYRK1A	Haspin	GSK3β	CK1ε	VEGFR2	ABL-1	JAK3	EGFR
1a	87	54	89	42	83	> 100	**37**	> 100	**3**	53	39	86
1b	> 100	92	96	93	89	> 100	71	74	> 100	95	68	92
1c	> 100	98	96	> 100	> 100	> 100	90	94	> 100	97	69	> 100
2a	> 100	93	> 100	100	> 100	95	88	79	47	92	69	98
3a	> 100	88	96	71	96	91	83	> 100	**7**	47	68	89
2aCl	90	95	80	90	81	> 100	91	83	**18**	99	65	92
2c	> 100	> 100	89	94	> 100	79	48	35	> 100	80	38	88
3c	1> 100	100	> 100	> 100	> 100	> 100	> 100	> 100	> 100	93	95	94
38a	84	42	45	97	> 100	94	74	> 100	93	> 100	99	93
38b	> 100	65	**28**	55	72	96	> 100	> 100	> 100	> 100	58	93
4a	> 100	73	> 100	> 100	100	80	41	89	**3**	92	49	93
5a	> 100	75	> 100	> 100	> 100	81	48	86	**21**	95	68	83

Table 2 Inhibitory activities of the first round of compounds against a short panel of disease-related protein kinases. The table displays the remaining kinase activities detected after treatment with 1 µM of the tested compounds. Results are expressed in % of maximal activity, i.e. measured in the absence of inhibitor but with an equivalent dose of DMSO (solvent of the tested compounds). ATP concentration used in the kinase assays was 10 µmol/L (values are means, n = 2). Kinases are from human origin unless specified: *Mm*, *Mus musculus; Rn, Rattus norvegicus*. Data obtained for regorafenib (**1a**) are colored in light grey.

Compd.	CDK5/p25	CDK9/CyclinT	PIM1	*Mm*CLK1	*Rn*DYRK1A	Haspin	GSK3β	CK1ε	VEGFR2	ABL-1	JAK3	EGFR
1a	> 100	85	> 100	> 100	> 100	> 100	86	> 100	50	99	74	91
1b	> 100	94	> 100	> 100	> 100	84	> 100	94	> 100	97	79	90
1c	> 100	91	> 100	> 100	90	> 100	85	95	82	90	84	99
2a	> 100	> 100	> 100	> 100	> 100	> 100	90	97	61	> 100	83	96
3a	> 100	> 100	> 100	> 100	> 100	> 100	83	98	**11**	99	68	97
2aCl	> 100	> 100	100	> 100	> 100	> 100	95	> 100	> 100	100	68	98
2c	> 100	> 100	> 100	> 100	96	> 100	98	84	88	> 100	73	98
3c	> 100	96	> 100	> 100	> 100	> 100	94	90	> 100	95	87	84
38a	> 100	74	81	> 100	> 100	> 100	85	> 100	> 100	> 100	78	91
38b	> 100	100	92	> 100	> 100	> 100	> 100	> 100	66	> 100	73	94
4a	> 100	99	> 100	> 100	> 100	99	81	86	**8**	92	78	> 100
5a	> 100	81	> 100	> 100	> 100	> 100	95	98	47	95	82	83

The higher activity of **3a** when compared to **2a** could result from a higher degree of freedom to fit the bulky ferrocene core into the hydrophobic pocket of VEGFR2 while it is known that 2-halogenated-5-(trifluoromethyl)phenyl-1-ureido rings are highly potent kinase inhibitors,[22] thus explaining the activity of **2aCl**. As already observed with compound **1c**, the ferrocene oxamides **2c** and **3c** were ineffective to inhibit VEGFR2, as well as the truncated analogs **38a-b**. However, the ferrocene-based carboxamides **4a** and **5a** show promising inhibitory activity, the former being even more efficient at a 1 µM concentration when compared to regorafenib (**1a**). Interestingly, most of the new compounds acting as potent inhibitors of VEGFR2 show only weak inhibition properties for the other tyrosine kinases tested (ABL-1, JAK3 and EGFR). Only **1a** and the ferrocene oxamide **2c** were moderately active against JAK3 when tested at 10 µM.

Ultimately, we calculated the IC_{50} values for the most promising compounds, thus establishing the ferrocenic derivatives **3a**, **4a** and **5a** as effective VEGFR2 inhibitors with micromolar values (Table 3). Therefore, these results show that ferrocene ureas and carboxamides can behave as effective and selective inhibitors of VEGFR2, validating our approach to target angiogenesis processes.

Table 3 Selected IC_{50} values (µM) for compounds of Table 1.

Entry	**Product**	VEGFR2
1	**1a**	1.72
2	**2aCl**	2.73
3	**3a**	0.35
4	**4a**	0.78
5	**5a**	0.55

Cellular assays.

While no original target could be identified for the newly prepared regorafenib analogues, a promising activity was noticed on VEGFR2, one of the primary targets of regorafenib. Therefore, we also evaluated the effect of our compounds on the viability of colorectal cancer cell lines. HCT116 cells were exposed to the new compounds in various conditions: 15 µM for 24h (Fig 5, blue bar) or 5 µM for 48 or 72h (Fig 5, orange and green bars, respectively), and cell viability was assessed using the MTT test. At 15 µM for 24h, the squaramide **1b** was found to be more potent when compared to regorafenib (**1a**) while a marked loss of activity was noticed for the ferrocene derivatives **2a** and **3a**. Furthermore, the chloroferrocene derivative **2aCl** was found to be as active as **2a** although it was previously shown to be a more active VEGFR2 inhibitor (Table 1). However, moving from the urea to the oxalic amide derivatives was accompanied by a reduced viability when the cells were incubated in the presence of **2c** and **3c**. The derivatives **4a** and **5a** with the ferrocene moiety attached to the pyridinecarboxamide were almost inactive. At lower concentrations for prolonged incubation time (Fig 7, orange and green bars), compound **1b** remained the more potent analogue, as effective as regorafenib (**1a**) at 5 µM after 72h. The ferrocene derivatives **2a**, **3a** and **2aCl** were always less active than the parent drug while **3c** was found to be more active when compared to **2c**. We were glad to observe that while compounds **4a** and **5a** were unable to effectively reduce cell viability at 15 µM, prolonged incubation time at lower concentration restored their activity and **4a** was even found as efficient as **1a** after 72h. The truncated analogs of regorafenib, the urea **38a** and the squaramide **38b**, were generally less active than their reference compounds, clearly indicating that the pyridine ring is of main importance due to its ability to interact with the ATP binding site of the kinases.

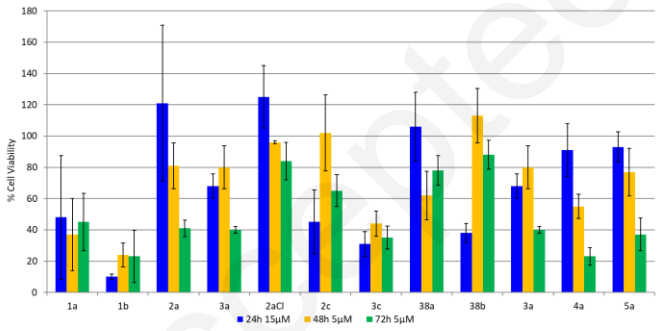

Fig 7. Viability of HCT116 cells using the MTT assay. Cell viability (% of control) was measured using the MTT test after exposure of the HCT116 cells to the selected compounds at the concentrations and time indicated. Mean values of three experiments, except for **1b** and **2a** for 24h and **2aCl** for 24-72h with two assays.

From these first cellular assays results, it appears that the high activity of compound **1b**, taken together with few other reported examples of squaramide-based anticancer molecules,[85-87] tends to validate the use of this polar group to reach potent kinase inhibitors. Surprisingly, while **1b** was unable to inhibit VEGFR2, it was found as the most active compound to reduce HCT116 cells viability. Therefore, it is reasonable to propose that other targets implicated in the colorectal cancer cells dynamics might be inhibited by this compound.

Concerning the ferrocene-based analogues of **1a**, they were globally less active than the reference drug. While the use of a methyl spacer between the ferrocene and the urea was without effect (compound **2a** vs **3a**), a marked effect was noticed in the oxalic amide series, compound **3c** being more effective than **2c** to reduce cell viability, whatever the incubation conditions used. When compared to the other organometallic derivatives prepared, the higher degree of freedom in **3c** might ensure a better positioning of the bulky ferrocene into the hydrophobic pocket normally occupied by the (trifluoromethyl)phenyl ring. In the same vein of thought, the reduced ability of the chloroferrocene derivative **2aCl** to reduce cell viability when compared to **2a** might results from the higher steric bulk, incompatible with the pocket of the targeted kinases. A reverse effect was noticed with the ferrocene carboxamides **4a** and **5a**, the non-methylated one being slightly more active in all the incubation conditions tested. Indeed, as this part of the inhibitor is exposed to solvent in many of the kinases targeted,[88-90] it might be preferable for the lipophilic ferrocene not to be too exposed.

We finally selected a few compounds which were incubated at 5 µM for 24h with the less sensitive HT29 colorectal cancer cell line (Fig 8). On these cells, the squaramide **1b** was found to be less effective to reduce cell viability when compared with **1a** while the ferrocene analogue **2a** was as effective. The ferrocene oxamide **2c** and the truncated squaramide **38b** were both found ineffective.

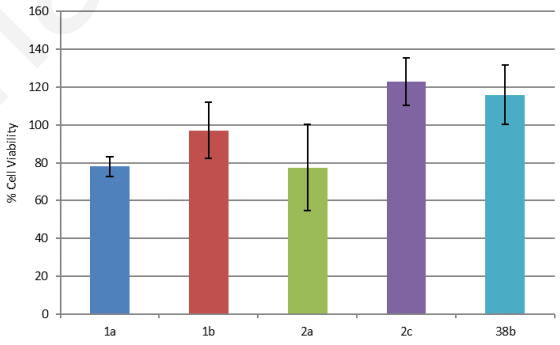

Fig 8. Viability of HT29 cells using the MTT assay. Cell viability (% of control) was measured using the MTT test after exposure of the HT29 cells to 5 µM of the selected compounds for 24h. Mean values of three experiments.

Intrigued by the results of **1b**, we next performed a dose-dependent activity study from 1 to 20 µM for compounds **1a**, **1b** and the truncated analog **38a**, all incubated for 24h (Fig 9). At 1 and 5 µM, almost no inhibition was noticed for **1a** and **1b** while **38b** tends to promote the cell viability. However, upon increasing the concentration of the inhibitor, **1b** was found to be more active when compared to **1a**, thus confirming the results obtained on the HCT116 cell line. As already observed on HCT116 cells, low activity of **38b** was also noticed in this cell line. Based on the above results, compounds **3c** and **1b** were found to be able to reduce colorectal cancer cells viability to a considerable extent. Therefore, their LD_{50} on the two cell lines considered were determined. While close values were recorded for regorafenib (**1a**, see ESI), compound **1b** was slightly more active on HCT116 cells than on the HT29 line (5 and 9 µM, respectively, see ESI). Interestingly, a 1 µM value was obtained

for compound **3c** LD_{50} on the HCT116, while HT29 cells proved to be much more resistant toward this compound (see ESI).

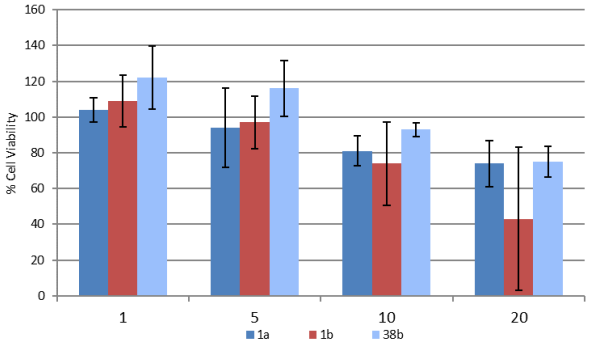

Fig 9. Viability of HT29 cells using the MTT assay. Cell viability (% of control) was measured using the MTT test after exposure of the HT29 cells to the selected compounds at the indicated concentrations (µM) for 24h. Mean values of three experiments.

While examples of biologically active 1,2-disubstituted ferrocene derivatives are scarce in the literature,[27, 83, 91-94] to the best of our knowledge, **2aCl** represents the first example of 2-substituted chloroferrocene derivative evaluated in both kinase and cellular assays. Thus, although it was barely able to reduce HCT116 viability, we were eager to compare its activity against regorafenib in a dose-dependent study. Therefore, HCT116 and HT29 cells were incubated with the two compounds at 5, 15 and 25 µM for 24 to 72h. As previously observed, whatever the conditions tested, **2aCl** was not able to reduce HCT116 cells viability to an appreciable extent (Fig 10). Although it needed 72h of incubation to reach around 80% of cell viability at 5 and 15 µM, the same value was obtained after 48h at 25 µM and did not evolve afterwards. Results were more encouraging on HT29 cells with the reduction of their viability evolving over 72h for the three concentrations used (Fig 11). Although clearly not as efficient as regorafenib (**1a**), a moderate 25% of viability was reached after 72h at 15 and 25 µM.

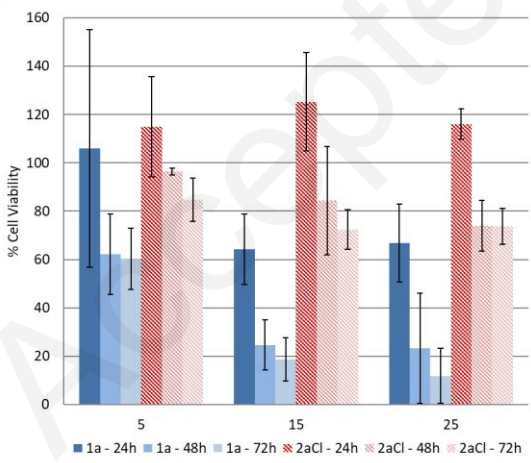

Fig 10. Viability of HCT116 cells using the MTT assay. Cell viability (% of control) was measured using the MTT test after exposure of the HCT116 cells to **1a** and **2aCl** for 24 to 72h at the indicated concentrations (µM). These data are representative of two experiments with similar results.

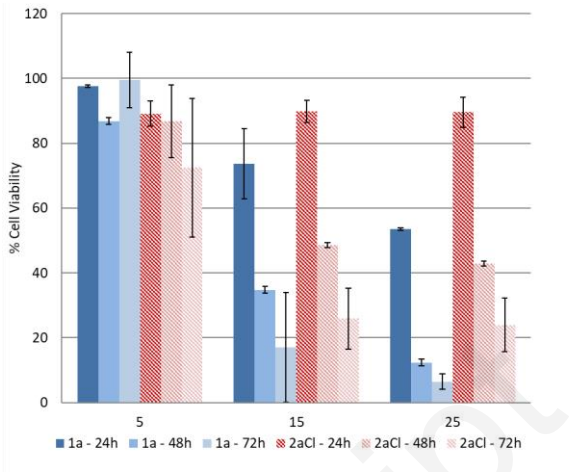

Fig 11. Viability of HT29 cells using the MTT assay. Cell viability (% of control) was measured using the MTT test after exposure of the HT29 cells to **1a** and **2aCl** for 24 to 72h at the indicated concentrations (µM). These data are representative of two experiments with similar results.

The selectivity of the new analogues for cancer cell lines was finally evaluated by exposing HEK293 non-cancer cells to various concentrations of the inhibitors. While the squaramide-based inhibitor **1b** was moderately selective for cells HCT116 at concentrations below 10 µM, the ferrocene derivative **3c** was selective for all the concentrations tested (see ESI). However, we were pleased to observe that both compounds **2aCl** and **3a**, although not the most active, showed a promising selectivity for cancer cells as compared to non-cancer ones over the whole range of evaluated concentrations (Fig. 12 and 13). As noticed previously (Fig 10 and 11), compound **2aCl** was found to be more able to reduce the viability of HT29 cells when compared with HCT116 ones (Fig 13), although the latter are usually more sensitive to the presence of an antiproliferative compound.

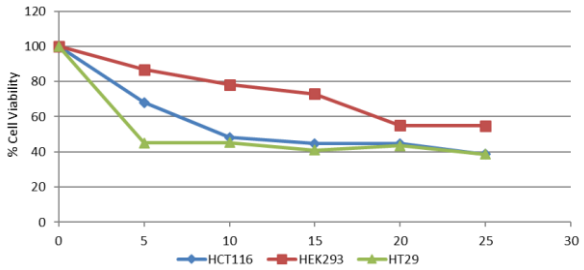

Fig 12. Viability of HCT116, HEK293 and HT29 cells using the MTT assay. Cell viability (% of control) was measured using the MTT test after exposure of the cells to **3a** for 48h at the indicated concentrations (µM).

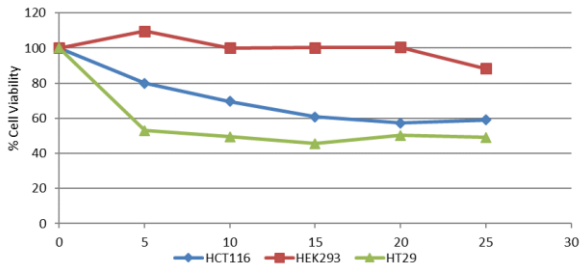

Fig 13. Viability of HCT116, HEK293 and HT29 cells using the MTT assay. Cell viability (% of control) was measured using the MTT test after exposure of the cells to **2aCl** for 48h at the indicated concentrations (µM).

Conclusions

Although small ferrocene-containing kinase inhibitors have been previously reported, the compounds prepared in the course of this study represent the first examples of complex ferrocene-based kinase inhibitors. From the cellular assays, the squaramide **1b** appeared as the most potent analogue to reduce cell viability although it was not able to inhibit VEGFR2. Therefore, the simple change of the traditional urea for a squaramide group has a profound impact on the biological target and suggests that **1b** might target other kinases implicated in colorectal cancer. Concerning the ferrocene derivatives, two compounds, namely **3c** and **4a**, emerged as promising to reduce HCT116 cell viability, the latter also being a good VEGFR2 inhibitor. Interestingly, the original chloroferrocene derivative **2aCl** was found promising in the HT29 cell line and features a promising selectivity for cancer cells, thus highlighting the importance of the substituent effect to reach biologically active products.

Conflicts of interest

Stéphane Bach is a founder and member of the scientific advisory board of SeaBeLife Biotech, which is developing novel therapies for treating liver and kidney acute disorders. This work was conducted in the absence of any commercial or financial relationships that could be construed as a potential conflict of interest.

Acknowledgements

This work was supported by the Région Bretagne (grant to M.W.), the Université de Rennes 1 and CNRS. We acknowledge the Fonds Européen de Développement Régional (FEDER; D8 VENTURE Bruker AXS diffractometer) and Rennes Métropole (HPLC acquisition). The authors also thank IBiSA (French Infrastructures en sciences du vivant: biologie, santé et agronomie) and Biogenouest (Western France life science and environment core facility network) for supporting the KISSf screening facility (FR2424, CNRS and Sorbonne Université), Roscoff, France. The authors would like to thank A. Bevillard for technical assistance and S. Ruchaud for her involvement in the KISSf platform. W. E. would like to thank Prof. F. Mongin for support, critically reviewing this document and making valuable suggestions.

Notes and references

1. *39-All-cancers-fact-sheet* - http://gco.iarc.fr/today/data/factsheets/cancers/39-All-cancers-fact-sheet.pdf.
2. L. Falzone, S. Salomone and M. Libra, *Frontiers in Pharmacology*, 2018, **9**, 1300.
3. J. Zhang, P. L. Yang and N. S. Gray, *Nat. Rev. Cancer*, 2009, **9**, 28-39.
4. P. Wu, T. E. Nielsen and M. H. Clausen, *Drug Discovery Today*, 2016, **21**, 5-10.
5. H. Daub, K. Specht and A. Ullrich, *Nat. Rev. Drug Discov.*, 2004, **3**, 1001-1010.
6. B. F., G. E. and P. G. J., *World J Clin Oncol* 2011, **2**, 80-93.
7. S. Wilhelm, C. Carter, M. Lynch, T. Lowinger, J. Dumas, R. A. Smith, B. Schwartz, R. Simantov and S. Kelley, *Nature reviews. Drug discovery*, 2006, **5**, 835-844.
8. S. Faivre, G. Demetri, W. Sargent and E. Raymond, *Nat. Rev. Drug Discov.*, 2007, **6**, 734-745.
9. H. Brenner, M. Kloor and C. P. Pox, *The Lancet*, 2014, **383**, 1490-1502.
10. E. Dekker, P. J. Tanis, J. L. A. Vleugels, P. M. Kasi and M. B. Wallace, *The Lancet*, 2019, **394**, 1467-1480.
11. S. M. Wilhelm, J. Dumas, L. Adnane, M. Lynch, C. A. Carter, G. Schütz, K.-H. Thierauch and D. Zopf, *Int. J. Cancer*, 2011, **129**, 245-255.
12. B. S., R. J. and D. A., *Gastrointestinal Cancer: Targets and Therapy*, 2014, **4**, 1-10.
13. H. Arai, F. Battaglin, J. Wang, J. H. Lo, S. Soni, W. Zhang and H.-J. Lenz, *Cancer Treatment Reviews*, 2019, **81**, 101912.
14. Y. Liu and N. S. Gray, *Nature Chemical Biology*, 2006, **2**, 358-364.
15. R. Roskoski, *Pharmacol. Res.*, 2016, **103**, 26-48.
16. C. J. W. W. F. Zhu, S. Xu, W. Li, H. H. Fang, Z. C. Chen, X. H. Tu, P. W. Zheng, *Advanced Materials Research*, 2014, **989-994**, 1048-1051.
17. B. R. Stockwell, S. J. Dixon and R. Skouta. WO2015051149, 2015.
18. A. T. Wecksler, S. H. Hwang, J.-Y. Liu, H. I. Wettersten, C. Morisseau, J. Wu, R. H. Weiss and B. D. Hammock, *Cancer Chemotherapy and Pharmacology*, 2015, **75**, 161-171.
19. M. Qin, S. Yan, L. Wang, H. Zhang, Y. Zhao, S. Wu, D. Wu and P. Gong, *European Journal of Medicinal Chemistry*, 2016, **115**, 1-13.
20. C.-Y. Liu, J.-C. Su, T.-T. Huang, P.-Y. Chu, C.-T. Huang, W.-L. Wang, C.-H. Lee, K.-Y. Lau, W.-C. Tsai, H.-P. Yang, C.-W. Shiau, L.-M. Tseng and K.-F. Chen, *Molecular Oncology*, 2017, **11**, 266-279.
21. S. Sun, J. Zhang, N. Wang, X. Kong, F. Fu, H. Wang and J. Yao, *Molecules*, 2018, **23**, 24.
22. M. Sonoshita, A. P. Scopton, P. M. U. Ung, M. A. Murray, L. Silber, A. Y. Maldonado, A. Real, A. Schlessinger, R. L. Cagan and A. C. Dar, *Nature Chemical Biology*, 2018, **14**, 291-298.
23. P. Le, E. Kunold, R. Macsics, K. Rox, M. C. Jennings, I. Ugur, M. Reinecke, D. Chaves-Moreno, M. W. Hackl, C. Fetzer, F. A. M. Mandl, J. Lehmann, V. S. Korotkov, S. M. Hacker, B. Kuster, I. Antes, D. H. Pieper, M. Rohde, W. M. Wuest, E. Medina and S. A. Sieber, *Nat. Chem.*, 2020, **12**, 145-158.
24. Q.-P. Qin, Z.-F. Wang, M.-X. Tan, S.-L. Wang, B.-Q. Zou, D.-M. Luo, J.-L. Qin and S.-H. Zhang, *Inorg. Chem. Commun.*, 2019, **104**, 27-30.
25. N. Metzler-Nolte, *Chimia*, 2007, **61**, 736-741.
26. *Ferrocenes: Ligands, Materials and Biomolecules*, Wiley, Chichester, 2008.
27. M. Navarro, W. Castro and C. Biot, *Organometallics*, 2012, **31**, 5715-5727.
28. M. Patra, G. Gasser and N. Metzler-Nolte, *Dalton Trans.*, 2012, **41**, 6350-6358.
29. G. Jaouen, A. Vessieres and S. Top, *Chem. Soc. Rev.*, 2015, **44**, 8802-8817.
30. M. Patra and G. Gasser, *Nat. Rev. Chem.*, 2017, **1**, 0066.
31. B. S. Ludwig, J. D. G. Correia and F. E. Kühn, *Coord. Chem. Rev.*, 2019, **396**, 22-48.
32. A. N. Nesmeyanov, L. G. Bogomolova and V. Viltcheskaya. US Patent 119 356, 1971.
33. S. Top, J. Tang, A. Vessieres, D. Carrez, C. Provot and G. Jaouen, *Chem. Commun.*, 1996, DOI: 10.1039/CC9960000955, 955-956.
34. Y. Wang, P. M. Dansette, P. Pigeon, S. Top, M. J. McGlinchey, D. Mansuy and G. Jaouen, *Chem. Sci.*, 2018, **9**, 70-78.

35. Y. Wang, F. Heinemann, S. Top, A. Dazzi, C. Policar, L. Henry, F. Lambert, G. Jaouen, M. Salmain and A. Vessieres, *Dalton Trans.*, 2018, **47**, 9824-9833.
36. Y. Wang, P. Pigeon, S. Top, J. Sanz García, C. Troufflard, I. Ciofini, M. J. McGlinchey and G. Jaouen, *Angew. Chem. Int. Ed.*, 2019, **58**, 8421-8425.
37. C. Biot, G. Glorian, L. A. Maciejewski, J. S. Brocard, O. Domarle, G. Blampain, P. Millet, A. J. Georges, H. Abessolo, D. Dive and J. Lebibi, *J. Med. Chem.*, 1997, **40**, 3715-3718.
38. F. Dubar, T. J. Egan, B. Pradines, D. Kuter, K. K. Ncokazi, D. Forge, J.-F. Paul, C. Pierrot, H. Kalamou, J. Khalife, E. Buisine, C. Rogier, H. Vezin, I. Forfar, C. Slomianny, X. Trivelli, S. Kapishnikov, L. Leiserowitz, D. Dive and C. Biot, *ACS Chemical Biology*, 2011, **6**, 275-287.
39. M. Patra, K. Ingram, V. Pierroz, S. Ferrari, B. Spingler, J. Keiser and G. Gasser, *J. Med. Chem.*, 2012, **55**, 8790-8798.
40. J. Hess, M. Patra, A. Jabbar, V. Pierroz, S. Konatschnig, B. Spingler, S. Ferrari, R. B. Gasser and G. Gasser, *Dalton Trans.*, 2016, **45**, 17662-17671.
41. J. Hess, M. Patra, V. Pierroz, B. Spingler, A. Jabbar, S. Ferrari, R. B. Gasser and G. Gasser, *Organometallics*, 2016, **35**, 3369-3377.
42. R. Rubbiani, O. Blacque and G. Gasser, *Dalton Trans.*, 2016, **45**, 6619-6626.
43. J. Hess, G. Panic, M. Patra, L. Mastrobuoni, B. Spingler, S. Roy, J. Keiser and G. Gasser, *ACS Infectious Diseases*, 2017, **3**, 645-652.
44. F. d'Orchymont, J. Hess, G. Panic, M. Jakubaszek, L. Gemperle, J. Keiser and G. Gasser, *MedChemComm*, 2018, **9**, 1905-1909.
45. K. Schlotter, F. Boeckler, H. Hübner and P. Gmeiner, *J. Med. Chem.*, 2005, **48**, 3696-3699.
46. N. Chavain, H. Vezin, D. Dive, N. Touati, J.-F. Paul, E. Buisine and C. Biot, *Molecular Pharmaceutics*, 2008, **5**, 710-716.
47. J. Amin, I. Chuckowree, G. J. Tizzard, S. J. Coles, M. Wang, J. P. Bingham, J. A. Hartley and J. Spencer, *Organometallics*, 2013, **32**, 509-513.
48. J. Amin, I. S. Chuckowree, M. Wang, G. J. Tizzard, S. J. Coles and J. Spencer, *Organometallics*, 2013, **32**, 5818-5825.
49. M. Tazi, W. Erb, Y. S. Halauko, O. A. Ivashkevich, V. E. Matulis, T. Roisnel, V. Dorcet and F. Mongin, *Organometallics*, 2017, **36**, 4770-4778.
50. W. Erb, J.-P. Hurvois, T. Roisnel and V. Dorcet, *Organometallics*, 2018, **37**, 3780-3790.
51. M. Tazi, M. Hedidi, W. Erb, Y. S. Halauko, O. A. Ivashkevich, V. E. Matulis, T. Roisnel, V. Dorcet, G. Bentabed-Ababsa and F. Mongin, *Organometallics*, 2018, **37**, 2207-2211.
52. W. Erb and F. Mongin, *Synthesis*, 2019, **51**, 146-160.
53. W. Erb and T. Roisnel, *Chem. Commun.*, 2019, **55**, 9132-9135.
54. W. Erb, T. Roisnel and V. Dorcet, *Synthesis*, 2019, **51**, 3205-3213.
55. M. Hedidi, G. Dayaker, Y. Kitazawa, Y. Tatsuya, M. Kimura, W. Erb, G. Bentabed-Ababsa, F. Chevallier, M. Uchiyama, P. C. Gros and F. Mongin, *New J. Chem.*, 2019, **43**, 14898-14907.
56. M. Tazi, W. Erb, T. Roisnel, V. Dorcet, F. Mongin and P. J. Low, *Org. Biomol. Chem*, 2019, **27**, 9352-9359.
57. W. Erb, L. Kadari, K. Al-Mekhlafi, T. Roisnel, V. Dorcet, P. Radha Krishna and F. Mongin, *Adv. Synth. Catal.*, 2020, **362**, 832-850.
58. M. Hedidi, W. Erb, G. Bentabed-Ababsa, F. Chevallier, L. Picot, V. Thiéry, S. Bach, S. Ruchaud, T. Roisnel, V. Dorcet and F. Mongin, *Tetrahedron*, 2016, **72**, 6467-6476.
59. M. Hedidi, J. Maillard, W. Erb, F. Lassagne, Y. S. Halauko, O. A. Ivashkevich, V. E. Matulis, T. Roisnel, V. Dorcet, M. Hamzé, Z. Fajloun, B. Baratte, S. Ruchaud, S. Bach, G. Bentabed-Ababsa and F. Mongin, *Eur. J. Org. Chem.*, 2017, **2017**, 5903-5915.
60. N. M. Brikci-Nigassa, G. Bentabed-Ababsa, W. Erb, F. Chevallier, L. Picot, L. Vitek, A. Fleury, V. Thiéry, M. Souab, T. Robert, S. Ruchaud, S. Bach, T. Roisnel and F. Mongin, *Tetrahedron*, 2018, **74**, 1785-1801.
61. R. Amara, H. Awad, D. Chaker, G. Bentabed-Ababsa, F. Lassagne, W. Erb, F. Chevallier, T. Roisnel, V. Dorcet, Z. Fajloun, J. Vidal and F. Mongin, *Eur. J. Org. Chem.*, 2019, **2019**, 5302-5312.
62. N. M. Brikci-Nigassa, L. Nauton, P. Moreau, O. Mongin, R. Duval, L. Picot, V. Thiéry, M. Souab, S. Ruchaud, S. Bach, R. Le Guevel, G. Bentabed-Ababsa, W. Erb, T. Roisnel, V. Dorcet and F. Mongin, *Bioorg. Chem.*, 2020, **94**, 103347.
63. F. Lassagne, C. Duguépéroux, C. Roca, C. Perez, A. Martinez, B. Baratte, T. Robert, S. Ruchaud, S. Bach, W. Erb, T. Roisnel and F. Mongin, *Org. Biomol. Chem*, 2020, **18**, 154-162.
64. N. A. Meanwell, *J. Med. Chem.*, 2011, **54**, 2529-2591.
65. U. Grädler, D. Schwarz, M. Blaesse, B. Leuthner, T. L. Johnson, F. Bernard, X. Jiang, A. Marx, M. Gilardone, H. Lemoine, D. Roche and C. Jorand-Lebrun, *Bioorg. Med. Chem. Lett.*, 2019, **29**, 126717.
66. H.-P. Buchstaller, M. Wiesner, F. Zenke, C. Amendt, M. Grell and C. Sirrenberg. WO2004085399, 2004.
67. A. C. Dar, R. L. Cagan, A. P. Scopton and M. Sonoshita. WO2018035346, 2018.
68. L.-M. Wang, B.-Q. Du, D.-Z. Zuo, M.-K. Cheng, M. Zhao, S.-J. Zhao, X. Zhai and P. Gong, *Res. Chem. Intermed.*, 2016, **42**, 3209-3218.
69. D. Bankston, J. Dumas, R. Natero, B. Riedl, M.-K. Monahan and R. Sibley, *Org. Process Res. Dev.*, 2002, **6**, 777-781.
70. R. Filler and H. Novar, *J. Org. Chem.*, 1961, **26**, 2707-2710.
71. C. Zhang, X. Tan, J. Feng, N. Ding, Y. Li, Z. Jin, Q. Meng, X. Liu and C. Hu, *Molecules*, 2019, **24**, 2108.
72. H. Liu, C. S. Tomooka, S. L. Xu, B. R. Yerxa, R. S. Sullivan, Y. Xiong and H. W. Moore, *Organic Syntheses*, 1999, **76**, 189.
73. A.-M. Liberatore, D. Pons, D. Bigg, G. Prevost and M.-C. Brezak Panetier. WO2009034258, 2009.
74. W. Erb, G. Levanen, T. Roisnel and V. Dorcet, *New J. Chem.*, 2018, **42**, 3808-3818.
75. L. Zhenteng, S. Lili and C. Zhicheng. CN108997209, 2018.
76. A. Kumar, N. Kumar, R. Sharma, G. Bhargava and D. Mahajan, *J. Org. Chem.*, 2019, **84**, 11323-11334.
77. C. L. Beck, S. A. Berg and A. H. Winter, *Org. Biomol. Chem*, 2013, **11**, 5827-5835.
78. S. Song, L. Qiang and H. Xiaolong. CN105330600, 2016.
79. P. Srinivas, S. Prabhakar, F. Chevallier, E. Nassar, W. Erb, V. Dorcet, V. Jouikov, P. Radha Krishna and F. Mongin, *New J. Chem.*, 2016, **40**, 9441-9447.
80. R. Sanders and U. T. Mueller-Westerhoff, *J. Organomet. Chem.*, 1996, **512**, 219-224.
81. J. W. Huffman, L. H. Keith and R. L. Asbury, *J. Org. Chem.*, 1965, **30**, 1600-1604.
82. *For an alternative protocol, see ESI.*
83. M. Patra, G. Gasser, M. Wenzel, K. Merz, J. E. Bandow and N. Metzler-Nolte, *Organometallics*, 2012, **31**, 5760-5771.
84. S. Imstepf, V. Pierroz, R. Rubbiani, M. Felber, T. Fox, G. Gasser and R. Alberto, *Angew. Chem. Int. Ed.*, 2016, **55**, 2792-2795.
85. W. Mederski, U. Emde, G. Barnickel, F. Zenke, H. Greiner and F. Stieber. WO2007014608, 2007.
86. Q. Zhang, Z. Xia, M. J. Mitten, L. M. Lasko, V. Klinghofer, J. Bouska, E. F. Johnson, T. D. Penning, Y. Luo, V. L. Giranda, A. R. Shoemaker, K. D. Stewart, S. W. Djuric and A. Vasudevan, *Bioorg. Med. Chem. Lett.*, 2012, **22**, 7615-7622.
87. P. Villalonga, S. Fernández de Mattos, G. Ramis, A. Obrador-Hevia, A. Sampedro, C. Rotger and A. Costa, *ChemMedChem*, 2012, **7**, 1472-1480.
88. M. McTigue, B. W. Murray, J. H. Chen, Y.-L. Deng, J. Solowiej and R. S. Kania, *Proceedings of the National Academy of Sciences*, 2012, **109**, 18281-18289.

89. P. T. C. Wan, M. J. Garnett, S. M. Roe, S. Lee, D. Niculescu-Duvaz, V. M. Good, C. G. Project, C. M. Jones, C. J. Marshall, C. J. Springer, D. Barford and R. Marais, *Cell*, 2004, **116**, 855-867.
90. *http://www.rcsb.org/structure/6JOK*.
91. A. R. Bhat, A. I. Bhat, F. Athar and A. Azam, *Helv. Chim. Acta*, 2009, **92**, 1644-1656.
92. D. Razafimahefa, D. A. Ralambomanana, L. Hammouche, L. Pélinski, S. Lauvagie, C. Bebear, J. Brocard and J. Maugein, *Bioorg. Med. Chem. Lett.*, 2005, **15**, 2301-2303.
93. L. Cunningham, Y. Wang, C. Nottingham, J. Pagsulingan, G. Jaouen, M. J. McGlinchey and P. J. Guiry, *ChemBioChem*, 2020, **21**, 2974.
94. B. Ferber, S. Top, A. Vessières, R. Welter and G. Jaouen, *Organometallics*, 2006, **25**, 5730-5739.